Polymer-capped gold nanoparticles by ligand-exchange reactions†

Simona Rucareanu,‡ Marco Maccarini,§ Jeffrey L. Shepherd¶ and R. Bruce Lennox*

Received 16th April 2008, Accepted 30th September 2008
First published as an Advance Article on the web 4th November 2008
DOI: 10.1039/b806375c

The thiol-for-DMAP (4-(*N*,*N*-dimethylamino)pyridine) exchange-reaction is demonstrated to be very effective in preparing polymer-capped gold nanoparticles. A number of PEO- and PS-capped gold nanoparticles are thus prepared using mild reaction conditions with a minimal amount of excess thiol ligand. Excellent thermal stability, retention of gold core size and morphology as well as very high surface grafting of the polymeric ligand on the gold core are features of this procedure.

Introduction

Recent applications of various forms of nano-sized gold (nanoparticles, nanorods, nanoplates, *etc.*) in biomedicine and materials science have triggered a need for accessible preparation methods.[1–4] The design and synthesis of ligand-capped gold nanoparticles (Au NPs) however remains a challenge. Two factors need to be considered when designing Au NPs: good chemical/biological stability and appropriate functionalization. Both factors are finely controlled through the choice of capping ligand. Polymeric ligands are particularly valuable due to the opportunities they offer in terms of both stability and functionalization.[5–8] The present work focuses on the preparation of polymer-coated gold nanoparticles using the ligand-exchange procedure previously reported for shorter-chain (up to C16) thiol-protected Au NPs. The two types of ligand investigated are representative of water and organic-soluble polymers: thiol-terminated poly(ethylene oxide) (n = 6, 45; PEO_6SH and $PEO_{45}SH$) and polystyrene (n = 16, 125; $PS_{16}SH$ and $PS_{125}SH$). The thiol group provides strong binding to the gold surface. Poly(ethylene oxide) is an attractive ligand for biological applications because of its well-known ability to suppress non-specific protein binding and its biocompatibility.[9–11] Polystyrene has been used as a matrix for inorganic–organic composites consisting of Au NPs either dispersed in the polystyrene matrix or attached to polystyrene beads.[12,13]

There are two techniques to prepare chemically-bound polymer–Au NPs: the "grafting-from" and "grafting-to" procedures. The "grafting-from" approach consists of binding a polymer initiator to the gold surface followed by polymerization.[14,15] While leading to very high grafting densities the procedure is limited to low-temperature polymerization conditions due to the thermal sensitivity of the gold–sulfur bond. The "grafting-to" technique can be performed in a one-step (direct synthesis)[5,16] or two-step (ligand-exchange) reaction.[6,7,11,17] The former has the drawback of providing little control over the nanoparticle size, shape, and dispersity because of the steric hindrance caused by the polymer chains. The latter avoids this disadvantage by using pre-synthesized gold nanoparticles. However, the most common ligand-exchange reactions use thiol-capped nanoparticles as the starting material. It is very difficult to control the composition of the final nanoparticle in this type of reaction. Thiol-for-thiol exchanges generally lead to mixed monolayers. Using Au NPs with kinetically labile ligands (citrate or tetraoctylammonium bromide (TOAB)) as the starting material for preparation of polymer-coated Au NPs offers a flexible approach to control the composition of the protecting shell contribution. Citrate–Au NPs are relatively monodisperse but are large (>10–15 nm metal core) and available only as a dilute solution. TOAB–Au NPs are smaller (3–6 nm metal core), fairly monodisperse, and soluble in organic solvents. Residual TOAB is however difficult to remove.[18] We have previously established an efficient ligand-exchange procedure for preparation of thiol-protected Au NPs starting from 4-(*N*,*N*-dimethylamino)pyridine-capped gold nanoparticles DMAP-Au NPs.[19] The procedure was successfully applied to various short-chain thiols bearing different functionalities. The preparation of water- and organic-soluble polymer-coated Au NPs is explored here and a method which is both straightforward and reproducible is described.

Experimental

Chemicals

Hydrogen tetrachloroaurate trihydrate ($HAuCl_4 \cdot 3H_2O$, 99.9999%) was purchased from Strem Chemicals. Tetraoctylammonium bromide (TOAB, 98%), sodium borohydride ($NaBH_4$, 99%), 4-(*N*,*N*-dimethylamino)pyridine (DMAP, 99%) were received from Aldrich and used without further purification. $PS_{125}SH$ (M_n = 13 300, M_w/M_n = 1.7), PS_{2K} (M_W = 2400, M_n = 2100, M_W/M_n = 1.11, and PS_{84K} (M_W = 84 000, M_n = 81 000, M_W/M_n = 1.03 were available from previous studies.[16] $PS_{16}SH$ (M_n = 1660, M_w = 1830, M_w/M_n = 1.10) and $PEO_{45}SH$ (M_w = 2100) were purchased from Polymer Source, Montréal, Canada. PEO_6SH (M_w = 356.5, 98%) was received from

Department of Chemistry and Centre for Self-Assembled Chemical Structures, McGill University, 801 Sherbrooke St. West, Montreal, H3A 2K6, Quebec, Canada. E-mail: bruce.lennox@mcgill.ca

† Electronic supplementary information (ESI) available: ^{1}H-NMR spectra, stability, and TGA data of the polymer-capped nanoparticles. See DOI: 10.1039/b806375c

‡ Present address: TNO/Holst Centre, High Tech Campus 31, Eindhoven, 5656 AE, The Netherlands. E-mail: simona.rucareanu@tno.nl

§ Present address: Institut Laue-Langevin, BP 156, 6 Rue Jules Horowitz, 38042, Grenoble, Cedex 9, France. E-mail: maccarini@ill.fr

¶ Present address: Department of Chemistry and Biochemistry, Laurention University, Sudbury, P3E 2C6, Ontario, Canada. E-mail: jshepherd@laurentian.ca

Polypure, Oslo, Norway. PS_{25K} ($M_W = 25\,000$, $M_W/M_n = 1.06$) and PS_{50K} ($M_W = 50\,000$, $M_W/M_n = 1.06$) came from Alfa Aesar. PS_{100K} ($M_W = 100\,000$ $M_W/M_n = 1.04$) was a kind gift from Dr Adi Eisenberg of McGill University. TOAB–Au and DMAP–Au were synthesized using Caruso's procedure.[20] Sephadex G-50 (Sigma-Aldrich) was swollen in suitable solvents and loaded into a glass column. All solvents (ACS or spectroscopy grade) came from Fischer Scientific. Highly pure water with resistivity 18 MΩ was obtained by using a Milli-Q Water System (Millipore Corporation).

Instrumentation

UV-Vis spectra were recorded at room temperature with a Cary 5000 UV-Vis-NIR spectrophotometer (Varian Instruments) using 1 cm quartz cuvettes. ^{1}H-NMR spectra were obtained on a Varian 400 MHz instrument using D_2O or CD_2Cl_2 as solvent. Spectra are referenced to the residual protons in the deuterated solvent. Bright field TEM images were obtained using a Philips CM200 instrument operating at 200 kV. The samples were prepared by dropcasting a dilute solution containing the nanoparticles on a carbon-coated copper grid (400 Mesh) and allowing the solvent to evaporate. The 3″ × 4″ negatives were scanned at a resolution of 300 dpi using an Epson 1200 photo scanner and its negative adapter. The gold core diameter distribution was determined from the TEM images using in-house-developed image analysis software where at least 300 particles constitute a data set per sample. Weight fractions of polymer layer and gold were measured by thermal gravimetric analysis (TGA) performed on a TA instrument, Q500 model with two mass flow controllers. 5–10 mg of accurately weighed samples were run from room temperature to 550 °C under nitrogen (60 mL min^{-1}), then switched to air (60 mL min^{-1}), and run up to 700 °C at 20 °C min^{-1}. The TGA was calibrated using the Curie point of Ni wire.

Procedure

PEO_nS–Au NPs ($n = 6, 45$). In a typical synthesis 125 mL of PEO_nSH solution (0.45×10^{-3} M in 95% ethanol or Milli-Q water) was added to a 125 mL aqueous solution of DMAP–Au NP. The clear, burgundy red mixture was allowed to stand at room temperature overnight. Neither changes in color nor precipitation were observed. The clear burgundy solution was rotary evaporated and the reddish solid was taken up in a minimum volume of water and purified on a Sephadex G-50 column run under gravity flow. Elution with neutral water or water : acetone (1 : 1) yields PEO_nS–Au NP as a concentrated dark-red solution. Upon freeze-drying $PEO_{125}S$–Au NPs were obtained as a black, hygroscopic powder and PEO_6S–Au NPs as a black, hygroscopic, sticky powder.

$PS_{16}S$–Au NPs. In a typical synthesis 250 mL of $PS_{16}SH$ solution (0.45×10^{-3}M in dichloromethane–ethanol 2 : 1) was added to 250 mL aqueous solution of DMAP–Au NPs. The pH was adjusted to 5 with 20% acetic acid. The solution turned cloudy, then dark grey–blue and some precipitate formed. The mixture (one-phase) was allowed to stand at room temperature overnight. The mixture separated upon standing to form a clear, dark-red organic phase and a clear colorless aqueous phase. No precipitate was observed. The organic phase was isolated, washed several times with acidic water (pH 3, acetic acid) to remove the residual DMAP and freeze-dried. Upon freeze-drying from benzene 287 mg of $PS_{16}S$–Au NPs were obtained as a reddish-violet, fine powder.

$PS_{125}S$–Au NPs. In a typical synthesis 250 mL of $PS_{125}SH$ solution (0.45×10^{-3}M in dichloromethane–ethanol 2 : 1) was added to 250 mL aqueous solution of DMAP–Au NPs. Ethanol was further added until the mixture formed one-phase. The pH was adjusted to 5 with 20% acetic acid. The cloudy solution (one-phase) was allowed to stand at room temperature overnight. The solvent was rotary evaporated, the dark reddish-violet residue taken up in dichloromethane and washed several times with acidic water (pH 3, acetic acid) to remove the residual DMAP. Upon freeze-drying from benzene, 1.37 g of $PS_{125}S$–Au NPs were obtained as a dark reddish-violet, fine powder.

Results and discussion

DMAP–Au NPs are a versatile starting material for preparation of a large number of thiol-capped nanoparticles with the gold core size in the range of 4–6 nm.[19] Thiols with short and longer chains (up to C16) efficiently and quantitatively displace the DMAP under mild reaction conditions, while preserving the Au core size. The conditions previously established in our lab allow complete ligand-exchange with almost stoichiometric quantities of thiols. This is a considerable advantage when rare thiols are needed. It also circumvents purification difficulties associated with large excess of thiols.

PEO_nS–Au NPs ($n = 6, 45$)

Preparation and characterization. PEO_nSH thiols with 6 and 45 PEO units were assessed under the thiol-for-DMAP exchange conditions previously established.[19] When PEO_nSH is added to the aqueous solution of DMAP–Au NPs as an ethanol or aqueous solution, the reaction proceeds upon standing at room temperature for *ca.* 18 h. No precipitation and/or change of color occurs. From this we infer that this ligand-exchange reaction is not accompanied by side-effects such as irreversible aggregation or significant gold core size modifications. Aggregation is a major problem in ligand-exchange reactions involving Au NPs capped with weakly bound ligands. Au NP aggregation leads to loss of material and/or alteration of Au NP monodispersity. This arises mainly from a poor surface coverage of the gold by the incoming thiol or incomplete exchange. Generally, in order to avoid this problem, a large excess of incoming thiol is used. While reducing undesirable side-effects the use of excess of thiol poses considerable problems in the work-up and isolation of pure NPs. Previous work showed that performing the thiol-for-DMAP ligand exchange at pH 5 enables efficient ligand-exchange with only a small (*ca.* 10%) excess of quantity of incoming thiol.[19] This is effective because at pH 5 >99.9% of the outgoing DMAP is protonated (pK_a 9.55) and thus cannot compete with the incoming thiol for binding to the gold surface. However, in the case of the PEO_nSH the ligand-exchange proceeds smoothly and efficiently even at high pH ($pH_{DMAP–Au\ NPs} = 9–10$). This might

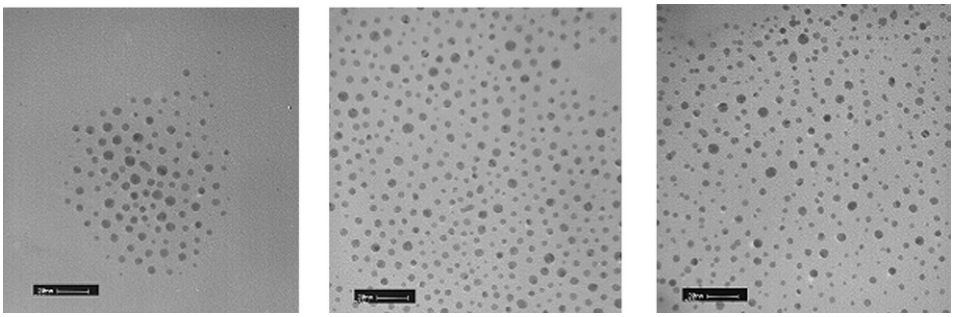

Fig. 1 TEM images of $PEO_{45}S$–Au NPs from batches of different sizes: 25 mL (left), 125 mL (centre), and 300 mL (right). Scale bar = 20 nm.

Table 1 Analytical data of PEO_nS–Au NPs

		Analytical data			
				TGA (%)	
NP sample	Batch size[a]/mL	λ_{max}/nm	Mean diameter metal core/nm	Organic	Gold
$PEO_{45}SAu$	25	516	4.9 ± 1.3	65.23	35.02
	125	514	4.1 ± 1.2	68.54	31.80
	125	514	4.6 ± 1.4	67.74	32.60
	300	516	4.1 ± 1.2	55.51[26]	44.49
	—	515	3.6 ± 1.2	29.30[16,21]	70.70
PEO_6SAu	125	513	4.0 ± 1.3	17.59	82.41

[a] Volume of DMAP–Au NPs (starting material, common concentration 3.6×10^{-7} M).

be due to the PEO adopting a rather extended conformation,[30] which allows formation of densely packed monolayers on the metal surface. Such a conformation will impede access of DMAP to the metal surface while also conferring increased thermodynamic stability to the newly formed nanoparticles. Additionally, water can also absorb on the PEO chains *via* hydrogen bonding[31] and thus hinder the access of DMAP to the gold surface. PEO_nS–Au NPs with a high degree of purity were obtained by gel permeation chromatography (GPC) on Sephadex-G50. Data obtained from UV-Vis spectra, TEM imaging (Fig. 1), and TGA measurements confirm that the procedure is reproducible even for batches of different size and can be readily scaled-up (Table 1).

Freeze-drying of PEO_nS–Au from water leads to a hygroscopic reddish-black powder that can be readily and completely redissolved in hydrophilic (water, dilute ethanol, acetone) or hydrophobic solvents (dichloromethane, toluene). This represents a convenient means to preserve these Au NPs for long periods of time and also offers control over the use of Au NPs. Data summarized in Table 2 shows that the preparation procedure is efficient and about 70% of the thiolated poly(ethylene oxide) used is found in the capping layer of the final Au NPs. The content of capping ligand ($PEO_{45}SH$) was calculated from the TGA data and the yield estimated based on the $PEO_{45}SH$ associated with the Au NPs.

Table 2 Overall efficiency of preparation of $PEO_{45}SAu$ NPs

	Starting materials		Final product		
Run	DMAP–Au NPs[a]/mL	$PEO_{45}SH$/mg	$PEO_{45}S$–Au NPs /mg (freeze dried)	$PEO_{45}SH$ content/mg	Yield (%)
1	25	24	28	18.3	76.2
2	125	118	120	82.2	69.7
3	125	118	125	84.7	71.3
4	300	284	400	222.0	78.2

[a] Aqueous solution, common concentration 3.6×10^{-7} M.

Stability. Samples of $PEO_{45}S$–Au NPs have been kept for several months at 4 °C both in solution and powder form (freeze-dried). The solutions remain clear, burgundy, and no precipitate forms. The freeze-dried samples completely redissolve in water or ethanol (70%) forming clear, red solutions. UV-Vis and TEM data (Table S1, ESI†) indicate no visible changes in NP gold core size or extent of polydispersity.

The thermal stability of $PEO_{45}S$–Au NPs was tested by heating an aqueous solution (0.2%) sequentially at 30, 40, 50, and 60 °C (1 h at each temperature), then overnight at 60 °C. TEM and UV-Vis data (Table S2, ESI†) indicate that $PEO_{45}S$–Au NPs are stable under moderate temperature conditions. Because PEO_nS–Au NPs are of great interest for biomedical applications that often require sterilization, we have also tested the stability of $PEO_{45}SAu$ NPs under harsh conditions used in sterilization procedures (autoclave: 122 °C; 18 psi; 45 min). Data obtained (Table S3, ESI†) indicate that no changes in NP gold core size occur upon autoclave sterilization under various conditions. $PEO_{45}S$–Au NPs thus prepared, proved to be very robust and stable even under harsh temperature (122 °C) and pressure conditions (18 psi). Decanethiol-capped Au NPs have been reported to increase size upon thermal treatment (100–115 °C for 30 min) from 1.5–2.5 nm to 4.7–5.7 nm.[28] On the other hand, gold nanoparticles heated under refluxing conditions (toluene ~120 °C) in the presence of excess capping ligand undergo size modifications resulting in more monodisperse smaller nanoparticles.[29] The process of digestive ripening was successfully applied to prepare nanoparticles with increased monodispersity. $PEO_{45}S$–Au NPs prepared from DMAP–Au NPs proved to be stable under similar thermal conditions with no significant changes in size or dispersity (Table S3, ESI†). We also note that the sterilized freeze-dried powder dissolves more readily in water compared to non-sterilized samples. The origins of this interesting observation are not yet understood.

Table 3 Comparison of grafting densities of PEO_nS–Au prepared by thiol-for-DMAP exchange and direct synthesis

		Grafting density/Å^2 per molecule	
Au NPs	Mean diameter/nm	Sphere[a]	Truncated octahedron[a]
$PEO_{45}SAu$	4.6 ± 1.4	11	14
$PEO_{45}SAu$[16]	3.6 ± 2.0	50	87
$PEO_{45}SAu$[16]	3.8 ± 1.0	83	102
PEO_6SAu	4.0 ± 1.3	18	22

[a] Surface area at the gold core if either a spherical geometry or more realistic truncated octahedron are assumed.

Grafting density. The grafting density is mainly determined by the chain conformation adopted by the polymer in the confined space surrounding the gold core. At low coverage on a 2D surface the PEO chains adopt a coiled conformation, the so-called "mushroom" regime. Increased coverage leads to more extended conformations of PEO in the "brush" regime.[22] Data obtained from TGA and TEM show a very high grafting density for both PEO_6SH and $PEO_{45}SH$. Small-angle neutron scattering measurements performed on $PEO_{45}SH$ are in good agreement with the TGA/TEM data.[25] The $PEO_{45}SH$ grafting density for the NPs prepared by this procedure is particularly high being 5–8 fold greater than in the case of Au NPs with similar gold core size prepared previously in our group by direct synthesis (Table 3).[16,21] For reasons not fully understood presently, the direct synthesis of $PEO_{45}SH$ from $HAuCl_4$ and $PEO_{45}SH$ with Superhydride (lithium triethylborohydride) in tetrahydrofuran yields nanoparticles with a significantly lower organic content (Table 1). For the shorter chain (PEO_6SH) the data obtained are in the same range as previously reported for alkyl thiols (21.4 Å^2 for $C_{12}SH$ assuming spherical geometry).[23]

Table 4 Analytical data of PS_nS–Au NPs

		Analytical data			
				TGA (%)[27]	
	Batch size[a]/mL	λ_{max}/nm	Mean diameter/nm	Organic	Gold
$PS_{125}SAu$	250	526	4.9 ± 1.3	90.06	9.92
	50	524	4.3 ± 1.4	86.05	13.95
$PS_{16}SAu$	250	529	4.5 ± 1.2	54.11	45.88
	125	527	4.0 ± 1.3	48.43	49.44

[a] Volumes of DMAP–Au NPs used as starting material.

PS_nS–Au NPs (n = 16, 125)

End-thiolated polystyrenes prove to be more difficult to graft to gold nanoparticles by ligand-exchange reaction with DMAP–Au NPs than thiolated poly(ethylene oxide)s. The complications are solubility related. Because thiolated poly(ethylene oxide) is extremely soluble in water and dilute ethanol, and the DMAP–Au NPs are also water soluble, the ligand-exchange takes place in one phase.

Thiolated polystyrene is of course very soluble in organic solvents but is immiscible with water, and the place-exchange takes place mainly at the interface of the two solutions. In the case of organic-soluble short-chain thiols there is no impediment to perform the ligand-exchange reaction in two-phase systems as the newly formed nanoparticles are readily transferred into the organic layer. But polystyrene is a bulky ligand and under the two-phase conditions tested the place-exchange either did not reach completion (after 48 h significant quantities of DMAP–Au NPs still remain in the aqueous phase) or is accompanied by aggregation leading to irreversible precipitation and thus, an important loss of material. Alternative solvents (toluene, toluene–acetone 1 : 2, dichloromethane, dichloromethane–ethanol 2 : 1, THF) did not yield acceptable results. However, addition of ethanol until the mixture becomes one phase, along with a lower reaction pH (pH 5) lead to an efficient ligand-exchange reaction. Analytical data (UV-Vis spectra and TEM images) obtained for the PS_nS–Au NPs thus prepared are presented in Table 4 and Fig. 2.

Thermal stability of PS_nS–Au NPs dispersed in polystyrene matrices. Polymer-coated Au NPs dispersed in homopolystyrene represent interesting composites.[24] Previous studies have shown that compatibility between the gold nanoparticles capping ligand and polymer matrix is a prerequisite for preparation of homogeneous composite in which Au NPs are thoroughly dispersed in the matrix.[24] For example short-chain alkyl thiol-capped Au NPs aggregate in medium/high molecular weight polystyrene matrices.[24] On the other hand both $PS_{16}S$–Au NPs and $PS_{125}S$–Au NPs readily disperse in a range of polystyrene matrices (PS_{2K}, PS_{25K}, PS_{50K}, PS_{84K}, PS_{100K}) by simply co-dissolution of the Au NP and the homoPS matrix in an appropriate solvent. Gentle shaking of the solution for a few

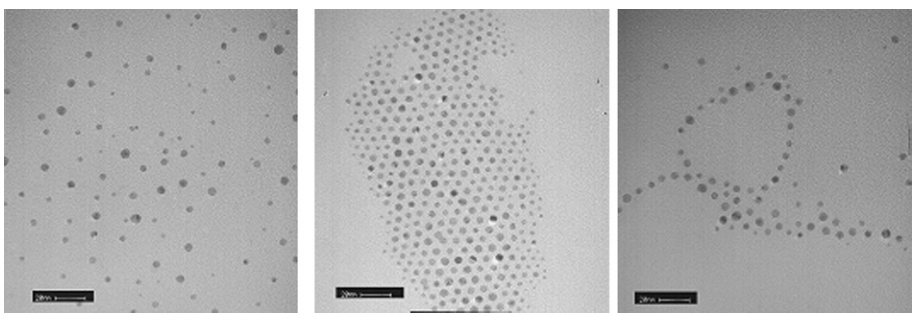

Fig. 2 TEM images of $PS_{16}S$–Au NPs (left), $PS_{125}S$–Au NPs (centre), composite $PS_{16}S$–Au NPs in PS_{25K} (right). Scale bar = 20 nm

minutes leads to a macroscopically homogeneous dark-red solution. Dichloromethane, tetrahydrofuran, and toluene can be used as solvents. TEM-images show that the gold nanoparticles do not aggregate and remain well dispersed in the polymer matrix (Fig. 2). These composites exhibit very good thermal stability. Samples of $PS_{16}S$–Au NPs embedded in PS_{25K} have been subjected to thermal treatment at high temperatures (140 °C; 160 °C) for various periods of time (1 h; 4 h, respectively). Both TEM and UV-Vis data collected for thermally treated samples (Table S4, ESI†) indicate that $PS_{16}S$–Au NPs dispersed into the polymer matrix are stable under these conditions.

Conclusions

Stable water- and organic-soluble polymer-capped Au NPs with very high grafting densities are readily and efficiently prepared by ligand-exchange reactions from DMAP–Au NPs by a two-step, grafting-to approach. The procedure described has several advantages. First, it preserves the size of the initial DMAP–Au NP core. Secondly, it can be applied to both water- and organic-soluble thiolated polymers. Thirdly, it requires only modest excess of thiolated polymers. Au NPs with very high grafting densities can thus be prepared with very good yields.

Acknowledgements

The authors are grateful to Dr Xue-Dong Liu of McGill Physics for assistance with TEM images and Petr Fiurasek of CSACS for the TGA data. Yolande Bastien of Physiology Department of McGill University is gratefully acknowledged for performing the sterilization measurements.

References

1 R. K. Visaria, R. J. Griffin, B. W. Williams, E. S. Ebbini and J. C. Bischof, *Mol. Cancer Ther.*, 2006, **5**, 1014–1020.
2 A. J. Reynolds, A. H. Haines and D. A. Russell, *Langmuir*, 2006, **22**, 1156–1163.
3 S. Kumar, N. Harrison, R. Richards-Kortum and K. Sokolov, *Nano Lett.*, 2007, **7**, 1338–1343.
4 A. C. Balazs, T. Emrick and T. P. Russell, *Science*, 2006, **314**, 1107–1110.
5 H. Otsuka, Y. Akiyama, Y. Nagasaki and K. Kataoka, *J. Am. Chem. Soc.*, 2001, **123**, 8226–8230.
6 J. Li, C. F. Crasto, J. S. Weinberg, M. Amiji, D. Shenoy, S. Sridhar, G. J. Bubley and G. B. Jones, *Bioorg. Med. Chem. Lett.*, 2005, **15**, 5558–5561.
7 D. Shenoy, W. Fu, J. Li, C. Crasto, G. Jones, C. Dimarzio, S. Sridhar and M. Amiji, *Int. J. Nanomed.*, 2006, **1**, 51–58.
8 A. H. Latham and M. E. Williams, *Langmuir*, 2006, **22**, 4319.
9 T. R. Tshikhudo, Z. Wang and M. Brust, *Mater. Sci. Technol.*, 2004, **20**, 980–984.
10 M. S. Nikolic, M. Krack, V. Aleksandrovic, A. Kornowski, S. Förster and H. Weller, *Angew. Chem., Int. Ed.*, 2006, **45**, 6577–6580.
11 D. Kim, S. Park, J. H. Lee, Y. Y. Jeong and S. Jon, *J. Am. Chem. Soc.*, 2007, **129**, 7661–7665.
12 J. Ouyang, C.-W. Chu, D. Sieves and Y. Yang, *Appl. Phys. Lett.*, 2005, **86**, 123507, (123501–123503).
13 C. S. S. R. Kumar, M. Aghasyan, H. Modrow, J. Hormes and R. Tittsworth, *J. Metastab. Nanocryst. Mater.*, 2005, **23**, 343–346.
14 K. J. Watson, J. Zhu, S. T. Nguyen and C. A. Mirkin, *J. Am. Chem. Soc.*, 1999, **121**, 462–463.
15 H. Skaff, M. F. Ilker, E. B. Coughlin and T. Emrick, *J. Am. Chem. Soc.*, 2002, **128**, 5729–5733.
16 M. K. Corbierre, N. S. Cameron and R. B. Lennox, *Langmuir*, 2004, **20**, 2867–2873.
17 H. Yockell-Lelièvre, J. Desbiens and A. M. Ritcey, *Langmuir*, 2007, **23**, 2843–2850.
18 C. A. Waters, A. J. Mills, K. A. Johnson and D. J. Schiffrin, *Chem. Commun.*, 2003, 540–541.
19 S. Rucareanu, V. J. Gandubert and R. B. Lennox, *Chem. Mater.*, 2006, **18**, 4674–4680.
20 V. J. Gandubert and R. B. Lennox, *Langmuir*, 2005, **21**, 6532–6539.
21 M. K. Corbierre, *PhD Thesis*, McGill University, Department of Chemistry, Montreal, Canada, 2004.
22 V. Dixit, J. Van de Bossche, D. M. Sherman, D. H. Thompson and R. P. Andres, *Bioconjugate Chem.*, 2006, **17**, 603–609.
23 T. Yonezawa, K. Yasui and N. Kimizuka, *Langmuir*, 2001, **17**, 271–273.
24 M. K. Corbierre, N. S. Cameron, M. Sutton, S. G. J. Mochrie, L. B. Lurio, A. Rühm and R. B. Lennox, *J. Am. Chem. Soc.*, 2001, **123**, 10411–10412.
25 M. Maccarini, S. Rucareanu, G. Briganti, and R. B. Lennox, unpublished results.
26 The lower organic content is due to the lower purity of the batch $PEO_{45}SH$ used.
27 The samples were not purified by GPC and some free thiolated polystyrene is still present. The $P_{16}S$–Au NP batch in the last entry contains 2.47% solvent—Fig. S8 ESI.† The TGA data are within the instrument measuring precision.
28 C. J. Zhong, W. X. Zhang, F. L. Leibowitz and H. H. Eichelberger, *Chem. Commun.*, 1999, 1211–1212.
29 B. L. V. Prasad, S. I. Stoeva, C. M. Sorensen and K. J. Klabunde, *Chem. Mater.*, 2003, **15**, 932–942.
30 L. D. Unsworth, Z. Tun, H. Sheardown and J. L. Brash, *J. Colloid Interface Sci.*, 2005, **281**, 112–121.
31 Y. Aray, M. Marquez, J. Rodriguez, D. Vega, Y. Simon-Manso, S. Coll, C. Gonzales and D. A. Weitz, *J. Phys. Chem. B*, 2004, **108**, 2418–2424.

